Impaired learning resulting from Respiratory Syncytial Virus infection

Janyra A. Espinoza[a], Karen Bohmwald[a], Pablo F. Céspedes[a], Roberto S. Gómez[a,b], Sebastián A. Riquelme[a], Claudia M. Cortés[c], Javier A. Valenzuela[d], Rodrigo A. Sandoval[d], Floria C. Pancetti[d], Susan M. Bueno[a,b], Claudia A. Riedel[c,1], and Alexis M. Kalergis[a,b,e,1]

[a]Millenium Institute on Immunology and Immunotherapy, Departamento de Genética Molecular y Microbiología, Facultad de Ciencias Biológicas, Pontificia Universidad Católica de Chile, Santiago 8331010, Chile; [b]Institut National de la Santé et de la Recherche Médicale, Unité 1064, 44093 Nantes, France; [c]Millenium Institute on Immunology and Immunotherapy, Departamento de Ciencias Biológicas, Facultad de Ciencias Biológicas y Facultad de Medicina, Universidad Andrés Bello, Santiago 8370146, Chile; [d]Laboratorio de Neurotoxicología Ambiental, Departamento de Ciencias Biomédicas, Facultad de Medicina, Universidad Católica del Norte, Coquimbo 1781421, Chile; and [e]Departamento de Reumatología, Facultad de Medicina, Pontificia Universidad Católica de Chile, Santiago 8331010, Chile

Respiratory syncytial virus (RSV) is the major cause of respiratory illness in infants worldwide. Neurologic alterations, such as seizures and ataxia, have been associated with RSV infection. We demonstrate the presence of RSV proteins and RNA in zones of the brain—such as the hippocampus, ventromedial hypothalamic nucleus, and brainstem—of infected mice. One month after disease resolution, rodents showed behavioral and cognitive impairment in marble burying (MB) and Morris water maze (MWM) tests. Our data indicate that the learning impairment caused by RSV is a result of a deficient induction of long-term potentiation in the hippocampus of infected animals. In addition, immunization with recombinant bacillus Calmette–Guérin (BCG) expressing RSV nucleoprotein prevented behavioral disorders, corroborating the specific effect of RSV infection over the central nervous system. Our findings provide evidence that RSV can spread from the airways to the central nervous system and cause functional alterations to the brain, both of which can be prevented by proper immunization against RSV.

cognition | behavior | inflammation | LTP | LTD

Respiratory syncytial virus (RSV) is an enveloped virus with a negative-sensed, single-stranded RNA genome that encodes 11 proteins (1, 2). RSV is the most prevalent pathogen of the *Paramyxoviridae* family and is the leading cause of lower respiratory tract infection in infants worldwide. RSV infects more than 70% of children in the first year of life, and 100% of children by age 2 years (3, 4). Although most symptoms of RSV infection, such as bronchiolitis and pneumonia, are related to airway inflammation, several central nervous system (CNS) manifestations have been reported in ~2% of patients with RSV-associated bronchiolitis (5), including seizures, central apnea, lethargy, feeding or swallowing difficulties, muscular tone or strabismus abnormalities, cerebrospinal fluid (CSF) abnormalities, and encephalopathy (6–8). Recently, there has been an increase in the number of case reports on RSV-caused encephalopathy, highlighting the importance of these symptoms (9).

Previous clinical studies have suggested an association between neurological symptoms and RSV infection (6, 8, 10), and other studies have documented the presence of RSV and RSV-specific antibodies in the CSF of patients suffering from severe bronchiolitis (11, 12). However, the pathophysiological mechanism responsible for RSV-caused encephalopathy remains undefined.

Despite evidence demonstrating the presence of RSV in the CSF of infected children and CNS alterations resulting from severe respiratory infection by this virus, several aspects of RSV biology regarding the CNS, such as the entrance mechanism, localization, and spreading of RSV in the CNS and its associated tissues, remain obscure. Here, we evaluated whether RSV was able to access the CNS and cause cognitive sequelae using

BALB/c mice and Sprague-Dawley rats. Immunofluorescence and quantitative real-time RT-PCR assays revealed the presence of both RSV nucleoprotein (N) and genetic material in the brains of infected animals. Furthermore, after a single intranasal (i.n.) challenge, we established the kinetics for entry and spreading of RSV within the infected brain. To evaluate behavioral and cognitive alterations and other CNS sequelae resulting from RSV infection, we used the marble burying (MB) (13, 14) and Morris water maze (MWM) (15, 16) tests. Our results support a neurotropic behavior for RSV and specifically show that the virus translocates to different regions in the CNS. Interestingly, we found that RSV infection caused impaired learning in rats and mice.

Because altered MWM and MB tests are suggestive of hippocampal alterations (17, 18), we evaluated whether animals that had been infected with RSV showed impaired hippocampal synaptic plasticity. Electrophysiology experiments of long-term potentiation (LTP) and long-term depression (LTD) were performed to evaluate learning and memory storage (19). Furthermore, we found that protective anti-RSV T-cell immunity by recombinant bacillus Calmette–Guérin (rBCG-N) RSV vaccine (1) prevents virus spreading to the CNS and the neurological sequelae caused by RSV respiratory tract infection.

Results

RSV Reaches the CNS After Intranasal Inoculation. To evaluate infection of the CNS after viral pneumonia, BALB/c mice and Sprague-Dawley rats were instilled i.n. with either RSV or a noninfectious supernatant (i.e., mock), which was used as a negative control. After infection, disease progression was monitored by body weight loss, and airway inflammation was assessed by histopathology and flow cytometry (Fig. S1). At 1, 3, 7, and 10 days postinfection, the brain, lungs, olfactory epithelium, and blood were collected from infected and mock mice and analyzed by real-time RT-PCR for the detection of RSV N transcripts. As shown in Fig. 1, RSV-N transcripts were detected as soon as 3 d postinfection in the CNS of mice. Furthermore, viral spread occurred from the midbrain to the brainstem at day 7 (Fig. 1).

To clarify the possible entry pathway, we measured RSV RNA in the olfactory bulb, olfactory epithelium, and blood cells by real-time PCR. Viral genetic material was detected in olfactory

www.manaraa.com

Real-Time PCR Detection of RSV.
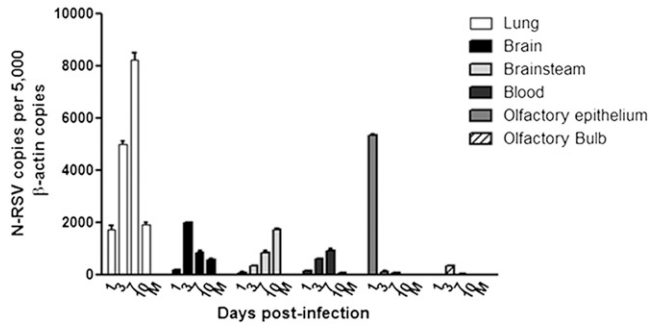
Fig. 1. Detection of RSV transcripts in the brain and blood of infected BALB/c mice. Data in the graph show the infection kinetics of RSV in the lung, blood, and CNS of infected mice at different times postinfection. Copy numbers for N transcripts normalized by 5,000 copies of a β-actin as housekeeping gene are shown. The peak of viral charge in brain was observed at day 3 postinfection, and the virus was able to spread to the brainstem in the following days.

epithelium as early as 24 h postinfection and in the olfactory bulb at 3 d postinfection. This result is consistent with previous studies showing RSV infection in human nasal epithelial cells (20, 21), which suggests that the olfactory epithelium is a primary target for RSV infection. In addition, similar experiments in RSV-infected rats were performed to evaluate disease parameters in airways and the CNS (Fig. S2). Conversely, RSV-N transcripts were detected in peripheral blood mononuclear cells (PBMCs) at 7 d postinfection, which is in accordance with previous reports (22, 23). Also, F protein expression was detected by flow cytometry in PBMCs isolated at days 3 and 7 postinfection (Fig. S3). Twenty-four hours after RSV challenge, both the F and N proteins of RSV were detected by immunofluorescence analyses in the olfactory bulb of infected, but not mock, mice (Fig. 2C). Starting at day 3 postinfection, disseminated staining for clustered viral proteins was observed in different anatomic areas of the brain

(Fig. 2 A–D). Finally, at day 7 postinfection, RSV was detected in the brainstem (Fig. 1).

Total F-RSV-associated fluorescence in both whole brain [cortex, hippocampus, ventromedial hypothalamic nucleus (VMH), and olfactory bulb] and whole lung (Fig. 2E) revealed F-RSV presence in RSV-infected mice (Fig. 2E). However, F-RSV levels were lower in the brain compared to the lungs. To establish whether RSV was present in other tissues not related with the CNS, we performed immunofluorescence for RSV F protein. As shown in Fig. S4, RSV F protein could not be detected in other organs after RSV infection. Altogether, real-time and immunofluorescence data support the notion of RSV as a unique neurotropic virus. Notably, the most infected areas in the brain were those adjacent to ventricles, including the third ventricle and the contiguous VMH. In addition, RSV was detected in other zones of the brain, including the hippocampus and cortex (Fig. 3).

We also evaluated whether RSV could use a so-called "Trojan horse" mechanism via the hematogenous pathway to enter and spread within the CNS. The Trojan horse mechanism refers to CNS viral entry via RSV-infected leukocytes that cross the blood–brain barrier. To test this, infected and mock mice were administered with a blocking antibody for CD49d i.v. before the infection. CD49d is expressed by these cells and is involved in the transendothelial migration of leukocytes into tissues that are undergoing inflammation (24, 25). CD49d antibody prevents the interaction of immune cells and endothelial cells, thereby reducing their translocation (24). As shown in Fig. 4, 3 d postinfection, the viral load is reduced in brain tissues in animals treated with CD49d. These data suggest that the hematogenous pathway is involved in RSV entry into the CNS; however, an alternative-pathway CNS RSV entry cannot be ruled out.

RSV Infection Causes Long-Term Learning Impairment. To evaluate the possible consequences of RSV infection in the CNS, the performance of control and RSV-infected BALB/c mice was evaluated by MB tests 30 d after viral challenge. Remarkably, mice infected with RSV 1 month before the test showed a significant impairment of MB behavior compared with control mice (Fig. 5 A and B). RSV-infected and control rats tested under similar experimental conditions (*SI Materials and Methods*)
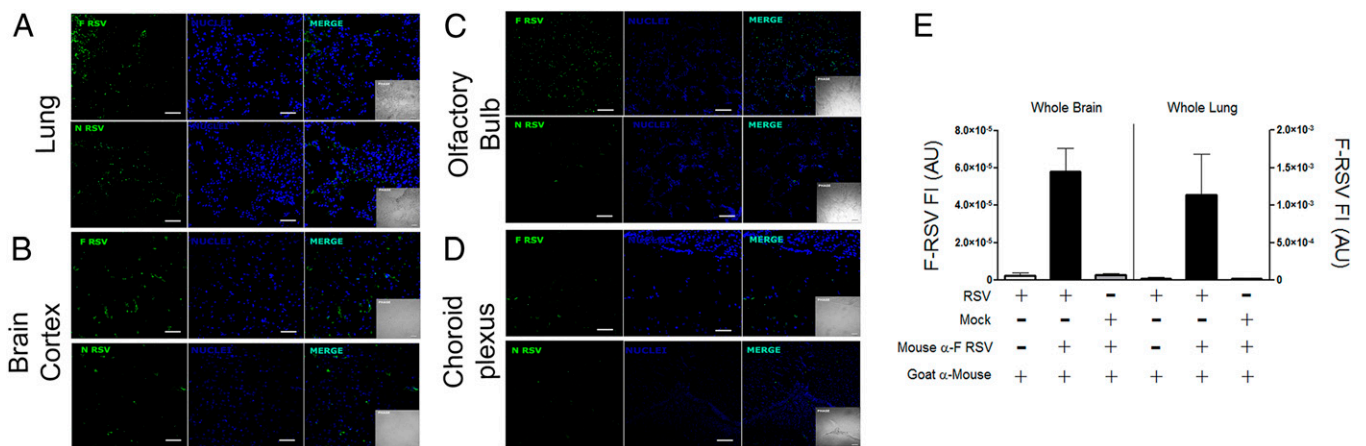
Fig. 2. RSV proteins were detected in lung and brain of infected mice. Confocal photomicrograph sections of lung and brain tissue. Viral proteins were observed by immunofluorescence (green fluorescence) in a confocal microscope using an anti-F-RSV or anti–N-RSV antibody. The nuclei were stained with thiazole orange-oligonucleotide conjugates (TOPRO-3) (blue). (A) Images of infected lung tissues 3 d after RSV infection. (*Upper*) Staining for F protein. (*Lower*) Staining for N protein. (B) Pictures of infected brain cortex 3 d after RSV infection. (*Upper*) Staining for F protein. (*Lower*) Staining for RSV Nucleoprotein. (C) Images of infected olfactory bulb tissues 1 d after RSV infection. (*Upper*) Staining for the F protein. (*Lower*) Staining for the nucleoprotein. (D) Images of infected choroid plexus after 3 d of RSV infection. (*Upper*) Staining for F protein. (*Lower*) Staining for N protein. (Scale bar, 150 μm.) (E) Quantification of total F-RSV channel fluorescence intensity per 40× field by pixel analysis of immunofluorescence for whole-brain and lung. Mouse α-F RSV, primary antibody; goat α-mouse, secondary antibody. More than 10 fields were analyzed per treatment.

Espinoza et al.
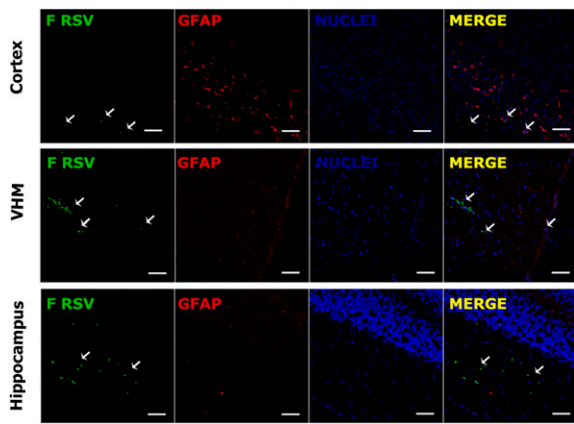
Fig. 3. Detection of F-RSV protein in specific brain regions. Confocal analyses were performed using tissue sections obtained from RSV-infected mice. Tissue was stained for nuclei (TOPRO-3; blue), GFAP (astrocyte marker; red), and F protein (RSV; green). Staining of brain tissue sections obtained at day 7 postinfection shows presence of viral protein adjacent to astrocytes zones. The white arrows show the clusters of RSV protein expression in the cortex, the VMH, and the hippocampus. (Scale bar, 150 μm.)

showed a similar impairment in MB behavior consistent with the effect observed in mice (Fig. S5).

We further evaluated cognitive function using the MWM test with RSV-infected Sprague-Dawley rats (26). One month after RSV infection, mock and virus-challenged rats were subjected to the MWM test (for further details, see *SI Materials and Methods*). Our results showed that infected rats displayed a significant increase in latency compared with mock control rats (Fig. 6A and Table S1). On the first day, RSV and control rats had latencies between 70 and 80 s (Table S1), indicating that none of the groups had swimming impediments. Importantly, between days 1 and 3, the group infected with RSV had significantly higher $P \leq 0.05$ latencies than the control group. However, by days 4 and 5 of the test, there were no significant differences between the latencies of RSV-infected and control animals. These data suggest that despite being infected 1 month before the assay, RSV-infected rats needed significantly more time and/or experience to learn the spatial cues required to find the hidden platform compared with control rats (Fig. 6A). It seems unlikely that the learning delay in RSV-infected rats was a result of visual perception defects because both RSV-infected and control rats showed equivalent latencies on MWM tests performed with a visible platform (cued-task training) (Fig. 6B). Therefore, normal visual perception of RSV-infected rats suggests that RSV infection may cause a long-lasting impairment in spatial learning capacity.

Learning Capacity Impairment Caused by Prior RSV Infection Is a Result of Reduced LTP. To determine how prior RSV infection impairs MWM and MB performance, we analyzed function of the hippocampus because of its direct role in the spatial learning and memory processes. Specifically, we focused on synaptic plasticity events occurring in the hippocampus, such as LTP and LTD. These two types of synaptic plasticity are generally considered the closest neural model for the cellular mechanism responsible for learning and memory storage. LTP experiments consisted of recording stimulus-evoked field responses [field excitatory postsynaptic potentials (fEPSPs)] at the stratum radiatum of CA1 of hippocampal slices that were obtained from control and previously infected rats (27). A 20-min stable baseline transmission was obtained and tested every 15 s. After baseline acquisition, the TBS was applied as described in *SI Materials and Methods*. After stimulation, data were acquired once every 15 s

for 1 h. Data from several experiments were compared according to the time of TBS stimulation for control and RSV-infected animals (Fig. 7B). For control rats, $176.4 \pm 16\%$ (Table S2) (SEM; $n = 5$), potentiation was achieved relative to the baseline. In contrast, for rats previously infected with RSV, potentiation was significantly reduced, at $138.4 \pm 4\%$ (Table S2) (SEM; $n = 7$). Representative traces of fEPSPs observed before and after LTP induction for control and RSV-infected animals are shown in Fig. 7C. These results indicate that RSV infection led to an impaired LTP response. Also, we evaluated LTP induction in the stratum pyramidale of CA1 of hippocampal slices and there were no differences between mock or infected animals (Fig. S6).

We also studied a second mechanism of synaptic plasticity known as LTD. To induce LTD, hippocampal slices received PBS stimulation 20 min after baseline (*SI Materials and Methods*). Our data show that RSV-infected animals demonstrated a significant impairment in the LTD response (Fig. 7D and Table S3). Impaired LTP and LTD responses were consistent with the increased latency shown by RSV-infected rats in MWM tests. These results support the hypothesis that rats previously infected with RSV are able to learn but require longer training periods compared with uninfected rats.

**CD49d Blockade Prevents the Behavioral Impairment Caused by RSV.** As shown in Fig. 4, treatment with anti-CD49d caused a significant viral load decrease in the brain of infected mice. We evaluated whether CD49d blockade protected against CNS alterations caused by RSV infection. BALB/c mice were given one or two doses of CD49d (70 μg) and then infected with the virus, as described in *SI Materials and Methods*. Thirty days postchallenge, MB tests were performed on control and anti-CD49d–treated mice. As shown in Fig. 8, mice that received the blocking antibody displayed normal MB behavior, despite RSV infection (Fig. 8). These results suggest that CD49d antibody blockade precludes RSV from entering the CNS, thereby preventing the deleterious effects of the virus on MB performance.

rBCG-N Vaccine Prevented RSV-Caused Damage to Airways and CNS. We have previously shown that immunization with live, attenuated BCG-N can protect against RSV-induced lung disease (28) (Fig. S7). To evaluate whether immunization with BCG-N could also induce an immune response capable of protecting against CNS infection by RSV, BALB/c mice were immunized with either BCG-N or BCG-WT and inoculated with RSV (*Materials and Methods*). Detection of RSV nucleoprotein transcripts was performed 3 d postinfection by real-time RT-PCR in the lungs and brains of infected mice. BCG-*N*-immunized mice showed significantly lower viral loads in both lungs and brain than did
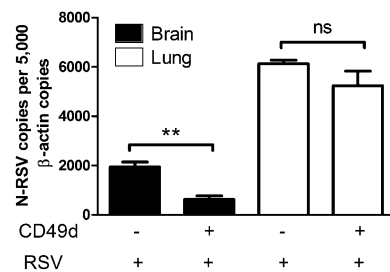
Fig. 4. Treatment with CD49d decreased CNS dissemination of RSV. BALB/c mice were infected intranasally with RSV and received a single dose of 70 μg anti-CD49d blocking antibody intravenously. Three days postinfection, mice were killed and the tissues prepared for RNA extraction. Data in the graph show the number of copies of RSV nucleoprotein transcripts in the brains of controls animals and animals treated with anti-CD49d antibody. Statistical analysis, one-way ANOVA; **$P < 0.05$, $n = 5$ per treatment.
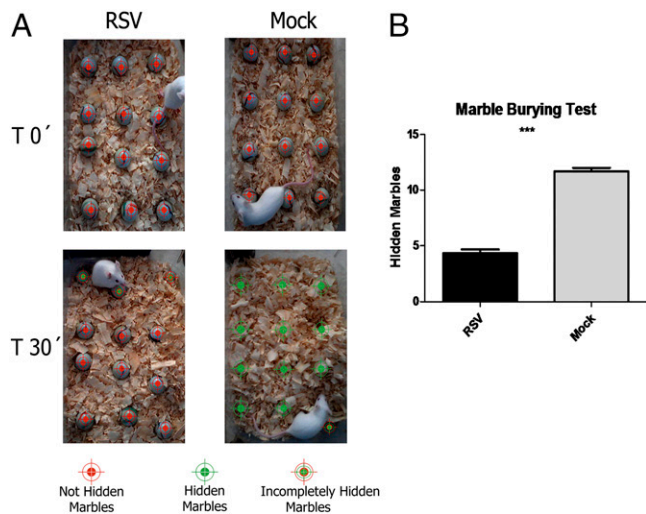
Fig. 5. RSV infection caused behavioral alterations. (A) Six-week-old BALB/c mice were challenged intranasally with RSV and 30 d later were subjected to MB tests to measure their cognitive capacity. The panels show representative images of MB tests for RSV-infected and control mice. (*Upper*) Initial position of marbles for RSV-infected and mock mice. (*Lower*) Position of the marbles 30 min after beginning the experiment. (B) Data in the graph show the quantification of hidden marbles for mock and RSV-infected mice. Statistical analysis, Student *t* test; ***$P < 0.0001$, $n = 10$ per treatment.

mice immunized with BCG-WT (Fig. 9A). We then performed MB tests 30 days postchallenge in vaccinated and control mice to evaluate whether immunization could prevent behavior impairment. BCG-*N*-immunized mice showed normal MB behavior despite RSV infection (Fig. 9B). These data suggest that immunization with BCG-N can confer an effective immune protection against RSV infection and respiratory disease, as well as preventing virus spread to the brain and RSV-induced CNS alteration.

Discussion

Recent studies have reported that RSV infection is associated with extrapulmonary manifestations, including cardiovascular, hepatic, and endocrine manifestations (8). In addition, RSV infection may lead to viremia, which can be critical because of systemic spreading to organs and tissues beyond the airways (8, 23, 26, 29).

Here, we evaluated whether RSV can reach CNS tissues after intranasal infection in mice and rats. We found that early after respiratory infection, RSV components reached the CNS, causing neurological impairment. The pattern of immunofluorescence staining for RSV F protein in the brain (focused) differed from that observed in infected lungs (disseminated). Furthermore, RSV proteins in the immediate vicinity of zones related to CSF production and blood vessels in the brains of infected mice. Neurotropic viruses can invade the CNS via two alternative pathways: through peripheral and cranial nerves axons or hematogenously (30, 31). The main hematogenous strategy is via infected phagocytes (Trojan horse mechanism) (32, 33). We evaluated this strategy by performing inhibition assays of leukocyte transendothelial migration to the brain parenchyma with a blocking antibody for CD49d (integrin α4). This molecule is expressed on most peripheral lymphocytes, thymocytes, and monocytes (24). The integrins mediate a variety of cell matrix interactions, recognizing the ligands VCAM-1 and fibronectin and regulating the transendothelial migration of leukocytes toward inflammation (24). Our data showed a reduction in the viral load in the brains of animals treated with the blocking antibody (Fig. 4). This suggests that RSV uses the hematogenous pathway associated with leukocytes (Fig. 4). Furthermore, we observed

that CD49d-blockade during the acute phase of the pulmonary disease prevented the alterations in MB behavior caused by RSV. However, two doses of anti-CD49d were required for protection (Fig. 8), suggesting that the blocking antibody might not completely prevent RSV entry into the CNS or that the antibody dose is not sufficient to block all of the receptors involved in leukocyte transmigration. This result suggests that the protection against RSV by CD49d blockade is a dose-dependent mechanism. Therefore, it is likely that the hematogenous pathway could be one of the mechanisms used by RSV to reach the CNS, which is consistent with the observation that virus antigens associate to ventricles and with the ability of RSV to infect mononuclear cells in the blood (Fig. S3).

Moreover, the kinetics of CNS infection suggests other possible mechanisms for RSV entry, such as anterograde transport via olfactory nerves. In fact, our results showed the presence of RSV in nasal epithelium the first day after infection, suggesting that the olfactory epithelium could be the primary target for RSV infection. This result is consistent with previous data that show RSV infection in human nasal epithelial cells (20, 21). The possibility of transport via olfactory nerves is consistent with the presence of viral antigens in olfactory bulb and telencephalon tissues as soon as 3 d postinfection, even before the detection of RSV in the blood.

Another important finding is the early infection of the brainstem, which may correlate with the development of RSV-associated apnea in children (34, 35). Our data suggest that RSV enters the CNS via hematogenous spread and by infection via neural transmission. Viral presence in the VMH could be related to the alterations in normal behavior in infected animals and decreased activity in children infected with the virus. The VMH is the brain region responsible for regulating food intake, glucose metabolism, and body weight (36). Our findings are consistent with RSV infection of the CNS; therefore, we evaluated the integrity of cognitive function in infected rodents by measuring behavior and learning. During RSV infection, MB and MWM tests performance was altered; therefore, these tests were carried out at least 30 d after infection to avoid a potential interference of the RSV-induced respiratory disease on the burying behavior and swimming capacities of the animals. MB is a rodent behavior test used to evaluate the behaviors of saving food and refuge from predators (13, 18). Lesions in the hippocampus cause an important decrease in the MB behavior, showing that these
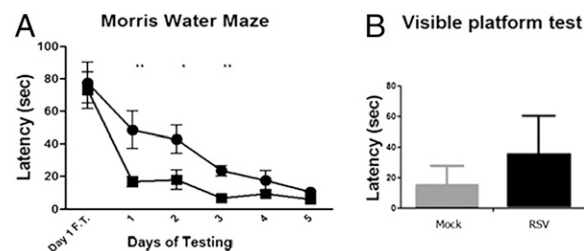

Fig. 6. RSV infection impaired learning and memory. Nine 3-wk-old Sprague-Dawley rats were i.n. challenged with RSV or vehicle; 30 d after the infections, rats were subjected to MWM tests to evaluate their cognitive capacity. (A) Data in the graph show the mean escape latency recorded from MWM test. Infected (●) and control (■) rats were subjected for 5 d to a MWM test. The day of each trial is indicated on the *X*-axis, and the mean ± SE escape latency is indicated on the *Y*-axis. The mean escape latency is the average of four trials performed on the day of the same experimental group. Statistical analysis (Mann–Whitney *U* test) showed significant differences on days 1, 2, and 3 with $P \leq 0.05$ ($n = 9$). (B) Mean escape latency from four trials for infected and control groups. Statistical analysis (unpaired *t* test) showed no significant differences between the control and infected animals.

NEUROSCIENCE
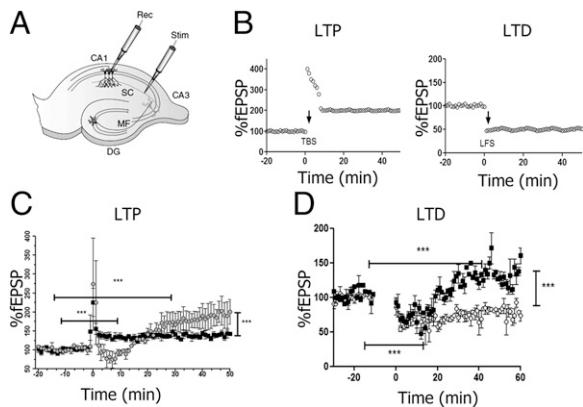
Fig. 7. Impaired synaptic plasticity resulting from RSV infection. (*A*) Rat hippocampal slice preparation and typical electrode placements for studying synaptic plasticity at SC synapses onto CA1, showing the regions CA1, CA3, and the DG. DG, dentate gyrus; MF, mossy fiber; SC, Schaffer collateral; Stim, stimulating electrode; Rec, recording electrode. (*B*) Illustration of LTP and LTD in the CA1 region of the hippocampus. (*C*) LTP in the stratum radiatum of the CA1 region of hippocampus. Synaptic strength, defined as the initial slope of the fEPSP (normalized to baseline), is plotted as a function of time. Data in the graph show the LTP induction elicited by high-frequency tetanic stimulation (100 Hz stimulation for 1 s) for RSV-infected (■) or mock control (●) rats. (*D*) LTD in the CA1 region of the hippocampus. Data in graph show the LTD elicited by low-frequency stimulation (5 Hz stimulation for 3 min given twice with a 3-min interval) for RSV-infected (■) or mock control (●) rats. (Scale bar, 0.5 mV, 10 ms.) Statistical analysis, unpaired *t* test; ***$P <$ 0.0001, *n* = 7 slides, 4 rats for each group.

instincts are controlled by this region (17, 37). Similar to MB, the MWM has proven to be a reliable test for measuring hippocampal synaptic plasticity and *N*-methyl-D-aspartate receptor function (38). Compared with control animals, both mice and
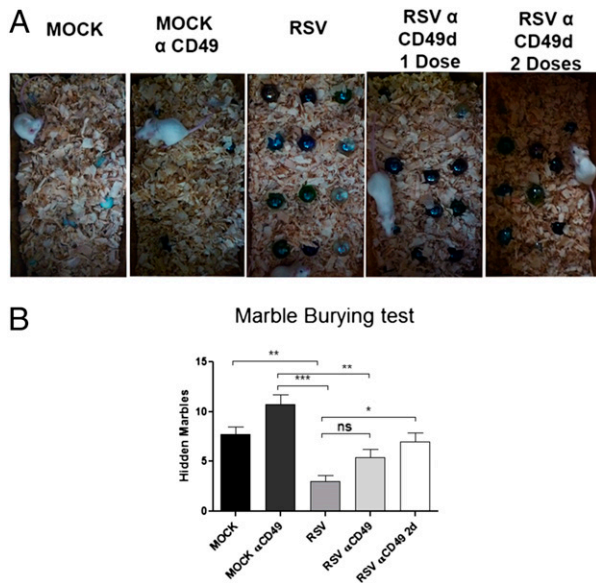
Fig. 8. CD49d blockade prevents the cognition impairment caused by RSV infection. Six-week-old BALB/c mice were treated with one or two doses of 70 μg anti- CD49d and i.n. inoculated with RSV or mock control. (*A*) Representative images of MB tests for each treatment. Mice receiving two doses of anti-CD49d showed no altered performance in MB tests after RSV infection in relation to control mice. (*B*) Data in the graph show the quantification of hidden marbles for all experimental groups. Statistical analysis, unpaired *t* test; ***$P <$ 0.0001, *n* = 5.
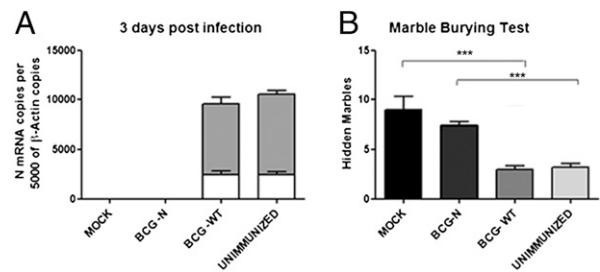
Fig. 9. Immunization with rBCG-N prevents the cognition impairment caused by RSV infection. Six-wk-old BALB/c mice were immunized with either rBCG-N or BCG-WT and intranasally inoculated with RSV or mock control. (*A*) Data in the graph show the viral load in lungs (gray bars) and brains (white bars) for unimmunized, rBCG-N-, and BCG-WT-immunized and uninfected mice. (*B*) Quantification of MB test for rBCG-N-, BCG-WT-immunized, and uninfected mice. Statistical analysis unpaired *t* test; ***$P <$ 0.0001, *n* = 10.

rats infected with RSV showed significant impairment in MB and MWM test performance, respectively. These data support altered hippocampal function.

Performance on MWM and MB tests has been associated with the efficiency and normal function of LTP and LTD (38). Therefore, we studied the synaptic plasticity in rats subjected to MWM. The results showed a significant decrease in the experimental LTP assay on the stratum radiatum in CA1 for rats previously infected with RSV. Interestingly, the LTP in stratum pyramidal was not affected (Fig. S6), suggesting that the impairment caused by RSV is limited to a specific zone in the dendrite of the neurons. Our findings suggest that RSV infection could alter LTP and LTD mechanisms, specifically at CA1 of hippocampus. This alteration in the LTP and LTD could be related to a reduction in synaptic plasticity and may result in low cognitive performance.

Although the mechanisms affecting synaptic plasticity remain unknown, it is possible that local activation of microglia, the production of inflammatory cytokines and oxidizing compounds, and an altered neurotransmitter secretion could all contribute to the cognitive impairment caused by RSV. To corroborate RSV as the cause of the observed neuropathology, we analyzed whether vaccination could prevent such alterations. Previously, our group showed that immunization with rBCG-N vaccine induced recruitment of CD4^{+} and CD8^{+} T cells to the lungs of RSV-infected mice and promoted efficient virus clearance without significant airway inflammation (1). Here, we observed that vaccination with rBCG-N protected mice from CNS RSV infection and, consequently, prevented alterations in the hippocampal function and allowed mice to display normal MB behavior even after RSV infection.

To the best of our knowledge, long-term functional alterations are seen in the CNS after RSV infection, which underscores the urgent need for safe and efficient RSV vaccines. To prevent CNS sequelae, candidate RSV vaccines must be capable of controlling RSV dissemination from the infected airways by eliciting an efficient and properly regulated T-cell immune response.

Materials and Methods

Animals and RSV Challenge. Four- to 6-wk-old female Balb/cJ WT mice and 3-wk-old female Sprague-Dawley rats were obtained from Jackson Laboratory and the central nurse-pond of the Pontificia Universidad Católica de Chile, respectively. Animals were maintained at the pathogen-free animal facility at the Pontificia Universidad Católica de Chile. All animal work was performed according to the respective biosafety committees of the Pontificia Universidad Católica de Chile and Universidad Andrés Bello. RSV was propagated over human epithelial cell line 2 (HEp-2) cells, as described in *SI Materials and Methods.* The RSV challenge was performed in a special room of the Public Health Institute of Chile. Animals were anesthetized with ketamine/xylazine (20 mg/kg and 1 mg/kg, respectively) and challenged i.n.

Espinoza et al.

www.manaraa.com

with 1×10^7 pfu of the RSV serogroup A, strain 13018–8. RSV is a clinical isolate provided by the Public Health Institute of Chile and was propagated over HEp-2 cells (*SI Materials and Methods*). As a control, noninfectious HEp-2 supernatant (mock) was instilled i.n. Body weight was determined daily after infection.

Mouse Immunization. rBCG-N was obtained as previously described (3). Five- to 6-wk-old BALB/c mice received a dorsal-flank subdermal injection with 1×10^8 cfu of either a Calmette–Guérin-WT bacillus or rBCG-N. After 10 d, mice received a booster with the respective BCG strain, as indicated earlier. Twenty-one days postimmunization, mice were challenged as described above. Body weight was determined daily after vaccination and during the days after infection.

Sample Collection. Mice and rats were killed at 1, 3, 7, and 10 days postinfection, and the lungs, brain, olfactory epithelium, and blood were obtained for quantitative real-time RT-PCR and immunofluorescence analyses. Specifically, the brain was dissected for separate analyses of the olfactory bulb, midbrain, and brainstem (medulla oblongata). The samples were analyzed by real-time RT-PCR and immunofluorescence, as described in *SI Materials and Methods*.

MWM Test for Spatial Learning and Memory. We performed the MWM test on 2-mo-old rats 30 d after RSV or mock challenge to assess neurological alterations in infected rats, as described in *SI Materials and Methods*.

MB Test for Limbic Behavior. To evaluate the object-hiding behavior of infected and control mice, we performed the MB test as described in *SI Materials and Methods*.

Extracellular Field Recording and LTP Induction. LTP and LTD assays from transverse hippocampal slides for RSV and mock rats was performed as described in *SI Materials and Methods*.

Inhibition of Leukocyte Transendothelial Migration. BALB/c mice were anesthetized with ketamine/xylazine and challenged i.n. with 1×10^7 pfu of RSV (mock animals received supernatants of uninfected HEp-2 cells). After infection, mice received 70 μg of anti-CD49d blocking antibody intravenously. Three days later, mice were killed, and the lungs and CNS tissues were collected for real-time PCR analyses. In addition, animals received either one dose at day 0 or two doses of anti-CD49d at day 0 and day 3 after challenge with RSV or mock. Thirty days later, mice were evaluated by MB tests.

1. Bueno SM, et al. (2008) Protective T cell immunity against respiratory syncytial virus is efficiently induced by recombinant BCG. *Proc Natl Acad Sci USA* 105(52):20822–20827.
2. Bueno SM, et al. (2008) Host immunity during RSV pathogenesis. *Int Immunopharmacol* 8(10):1320–1329.
3. González PA, Bueno SM, Riedel CA, Kalergis AM (2009) Impairment of T cell immunity by the respiratory syncytial virus: Targeting virulence mechanisms for therapy and prophylaxis. *Curr Med Chem* 16(34):4609–4625.
4. González PA, et al. (2008) Respiratory syncytial virus impairs T cell activation by preventing synapse assembly with dendritic cells. *Proc Natl Acad Sci USA* 105(39):14999–15004.
5. Sweetman LL, Ng YT, Butler IJ, Bodensteiner JB (2005) Neurologic complications associated with respiratory syncytial virus. *Pediatr Neurol* 32(5):307–310.
6. Millichap JJ, Wainwright MS (2009) Neurological complications of respiratory syncytial virus infection: Case series and review of literature. *J Child Neurol* 24(12):1499–1503.
7. Eisenhut M (2007) Cerebral involvement in respiratory syncytial virus disease. *Brain Dev* 29(7):454.
8. Eisenhut M (2006) Extrapulmonary manifestations of severe respiratory syncytial virus infection—a systematic review. *Crit Care* 10(4):R107.
9. Morichi S, et al. (2011) Classification of acute encephalopathy in respiratory syncytial virus infection. *J Infect Chemother* 17(6):776–781.
10. Zlateva KT, Van Ranst M (2004) Detection of subgroup B respiratory syncytial virus in the cerebrospinal fluid of a patient with respiratory syncytial virus pneumonia. *Pediatr Infect Dis J* 23(11):1065–1066.
11. Kho N, Kerrigan JF, Tong T, Browne R, Knilans J (2004) Respiratory syncytial virus infection and neurologic abnormalities: Retrospective cohort study. *J Child Neurol* 19(11):859–864.
12. Hirayama K, et al. (1999) Sequential MRI, SPECT and PET in respiratory syncytial virus encephalitis. *Pediatr Radiol* 29(4):282–286.
13. Deacon RM (2006) Digging and marble burying in mice: Simple methods for in vivo identification of biological impacts. *Nat Protoc* 1(1):122–124.
14. Dekeyne A, et al. (2012) S32212, a novel serotonin type 2C receptor inverse agonist/α2-adrenoceptor antagonist and potential antidepressant: II. A behavioral, neurochemical, and electrophysiological characterization. *J Pharmacol Exp Ther* 340(3):765–780.
15. Vorhees CV, Williams MT (2006) Morris water maze: Procedures for assessing spatial and related forms of learning and memory. *Nat Protoc* 1(2):848–858.
16. Morris R (1984) Developments of a water-maze procedure for studying spatial learning in the rat. *J Neurosci Methods* 11(1):47–60.
17. Jedynak P, et al. (2012) Lack of cyclin D2 impairing adult brain neurogenesis alters hippocampal-dependent behavioral tasks without reducing learning ability. *Behav Brain Res* 227(1):159–166.
18. Dekeyne A, et al. (2012) S32212, a novel serotonin type 2C receptor inverse agonist/α2-adrenoceptor antagonist and potential antidepressant: II. A behavioral, neurochemical, and electrophysiological characterization. *J Pharmacol Exp Ther* 340(3):765–780.
19. Neves G, Cooke SF, Bliss TV (2008) Synaptic plasticity, memory and the hippocampus: A neural network approach to causality. *Nat Rev Neurosci* 9(1):65–75.
20. Masaki T, et al. (2011) A nuclear factor-κB signaling pathway via protein kinase C δ regulates replication of respiratory syncytial virus in polarized normal human nasal epithelial cells. *Mol Biol Cell* 22(13):2144–2156.
21. Tsutsumi H, et al. (2011) Respiratory syncytial virus infection and the tight junctions of nasal epithelial cells. *Adv Otorhinolaryngol* 72:153–156.
22. Yui I, Hoshi A, Shigeta Y, Takami T, Nakayama T (2003) Detection of human respiratory syncytial virus sequences in peripheral blood mononuclear cells. *J Med Virol* 70(3):481–489.
23. Torres JP, et al. (2010) Respiratory syncytial virus (RSV) RNA loads in peripheral blood correlates with disease severity in mice. *Respir Res* 11:125.
24. Gan Y, Liu R, Wu W, Bomprezzi R, Shi FD (2012) Antibody to α4 integrin suppresses natural killer cells infiltration in central nervous system in experimental autoimmune encephalomyelitis. *J Neuroimmunol* 247(1-2):9–15.
25. Kawamoto E, Nakahashi S, Okamoto T, Imai H, Shimaoka M (2012) Anti-integrin therapy for multiple sclerosis. *Autoimmune Dis* 2012:357101.
26. Liu XM, Wang Z, Guo Y (2007) Respiratory syncytial virus nephropathy in rats. *Kidney Int* 71(5):388–396.
27. Kumar A (2011) Long-term potentiation at CA3-ca1 hippocampal synapses with special emphasis on aging, disease, and stress. *Front Aging Neurosci* 3:7.
28. Cautivo KM, et al. (2010) Efficient lung recruitment of respiratory syncytial virus-specific Th1 cells induced by recombinant bacillus Calmette-Guérin promotes virus clearance and protects from infection. *J Immunol* 185(12):7633–7645.
29. Rohwedder A, et al. (1998) Detection of respiratory syncytial virus RNA in blood of neonates by polymerase chain reaction. *J Med Virol* 54(4):320–327.
30. Mori I, Nishiyama Y, Yokochi T, Kimura Y (2005) Olfactory transmission of neurotropic viruses. *J Neurovirol* 11(2):129–137.
31. Weingartl H, et al. (2005) Invasion of the central nervous system in a porcine host by nipah virus. *J Virol* 79(12):7528–7534.
32. Kim WK, Corey S, Alvarez X, Williams K (2003) Monocyte/macrophage traffic in HIV and SIV encephalitis. *J Leukoc Biol* 74(5):650–656.
33. Pulzova L, Bhide MR, Andrej K (2009) Pathogen translocation across the blood-brain barrier. *FEMS Immunol Med Microbiol* 57(3):203–213.
34. Rayyan M, et al. (2004) Characteristics of respiratory syncytial virus-related apnoea in three infants. *Acta Paediatr* 93(6):847–849.
35. Seto M, et al. (1994) [Thirty seven cases of respiratory syncytial virus infection hospitalised and 7 severe cases with apneic attacks]. *Kansenshogaku Zasshi* 68(2):226–233.
36. Tran PV, et al. (2006) Diminished hypothalamic bdnf expression and impaired VMH function are associated with reduced SF-1 gene dosage. *J Comp Neurol* 498(5):637–648.
37. Bahi A, Dreyer JL (2012) Hippocampus-specific deletion of tissue plasminogen activator "tPA" in adult mice impairs depression- and anxiety-like behaviors. *Eur Neuropsychopharmacol* 22(9):672–682.
38. D'Hooge R, De Deyn PP (2001) Applications of the Morris water maze in the study of learning and memory. *Brain Res Brain Res Rev* 36(1):60–90.

NEUROSCIENCE

Espinoza et al.